Pole-piece Interactions with the Plasma in a Magnetic-layer-type Hall Thruster

IEPC-2017-426

Presented at the 35th International Electric Propulsion Conference
Georgia Institute of Technology • Atlanta, Georgia • USA
October 8 – 12, 2017

Hiroki Watanabe[1]
Tokyo Metropolitan University, Hino, Tokyo, 191-0065, Japan

Shinatora Cho[2]
Japan Aerospace Exploration Agency, Sagamihara, Kanagawa, 252-5210, Japan

Kenichi Kubota[3]
Japan Aerospace Exploration Agency, Chofu, Tokyo, 182-8522, Japan

Gen Ito[4] and Kenji Fuchigami[5]
IHI Corporation, Yokohama, Kanagawa, 235-8501, Japan

Yosuke Tashiro[6] and Shigeyasu Iihara[7]
IHI Aerospace Co., Ltd., Tomioka, Gunma, 370-2398, Japan

and

Ikkoh Funaki[8]
Japan Aerospace Exploration Agency, Sagamihara, Kanagawa, 252-5210, Japan

Abstract: With the growing interest in all-electric propulsion satellites, the demand for Hall thrusters has increased. Hence, the pole-piece interactions with the discharge plasma in a 2-kW-class magnetic-layer-type Hall thruster with an externally mounted hollow cathode were investigated, by isolating the surface material of each pole piece in the thruster exit plane from the thruster body. Graphite and boron nitride were employed as the pole-piece covers. The floating potentials on the graphite covers decrease with the increases in the anode mass flow rate and discharge voltage. Moreover, the negative potential on the outer cover is greater than that on the inner cover. The trends in the discharge behavior and thrust performance with respect to the magnetic field remain unaffected by the boundary conditions of the pole pieces, though they slightly affect the thrust performance when the magnetic field strength is maintained constant. The discharge current under the conductor condition is lower than that under the dielectric condition in most cases of the thruster configurations and operating conditions. In contrast to the discharge current behavior, the change in the boundary

[1] Assistant Professor, Department of Aerospace Engineering, hwatanabe@tmu.ac.jp.
[2] Researcher, Research and Development Directorate, choh.shinatora@jaxa.jp.
[3] Researcher, Aeronautical Technology Directorate, kubota.kenichi@jaxa.jp.
[4] Researcher, Research Laboratory, gen_ito@ihi.co.jp.
[5] Manager, Research Laboratory, kenji_fuchigami@ihi.co.jp.
[6] Engineer, Space Systems Department, yousuke-tashiro@iac.ihi.co.jp.
[7] Chief Engineer, shigeyasu-iihara@iac.ihi.co.jp.
[8] Associate Professor, Institute of Space and Astronautical Science, funaki.ikkoh@jaxa.jp.

condition tends to affect the thrust and specific impulse. However, changing the boundary condition from boron nitride to graphite improves the thrust-to-power ratio and anode efficiency in most cases, because of the considerable decrease in the discharge current.

Nomenclature

I_d	=	discharge current
I_{sp}	=	specific impulse
$\dot{m}_a$	=	anode mass flow rate
f_i	=	primary oscillation frequency
F/P	=	thrust-to-power ratio
L_d	=	length of ionization and acceleration regions
V_d	=	discharge voltage
V_i	=	accelerated ion velocity
V_n	=	thermal velocity of neutral propellant
Δ	=	oscillation amplitude
η_a	=	anode efficiency
τ	=	measurement time

I. Introduction

WITH the expectation that launch expenses can be controlled by reducing the satellite launch mass, all-electric propulsion satellites have received considerable attention. In Japan, the Japan Aerospace Exploration Agency, IHI Aerospace, and IHI Corporation have been currently pursuing research and development of a 6-kW-class Hall thruster to launch an all-electric propulsion satellite [1]. To develop Hall thrusters with a low-risk path towards flight, the interaction between the thruster system and a ground test facility needs to be studied. Recently, in addition to the ingestion of a propellant exhausted from a thruster, the electrical interaction between a ground-based vacuum chamber and the plasma produced by the thruster have been identified and discussed. McDonald [2] demonstrated that the thruster body current, flowing to the ground, was composed of electrons collected on the exposed metal components of the thruster, including that on the pole pieces. Goebel et al. [3] studied a magnetically shielded Hall thruster and identified the strong interactions between the pole pieces and the discharge plasma. In another study, Paterson et al. summarized the electrical configurations in relation to a conducting vacuum chamber and demonstrated that the boundary conditions of the exit plane and the electrical configuration of the thruster affected the thrust performance, discharge current oscillation, and plume characteristics [4].

Hence, the surface materials of the pole pieces and their electrical configurations are important factors in studying the thrust performance, discharge stability, and thruster lifetime. In previous studies, the surface material of the pole pieces had been electrically connected to the thruster body, when a conductor had been employed as the surface material. In this configuration, when the thruster body is isolated from the facility ground, the ion and electron currents flowing through the inner pole piece, outer pole piece, and thruster body are balanced such that the total current flowing to the ground is zero. This is because the current balance in this case is analogous to that in a floating Langmuir probe. Compared to the side surface of the thruster body, electrons can easily flow into the surface of inner and outer pole pieces because of the high electron temperature and strong magnetic field near the discharge channel. Thus, if the surface material of each pole piece is isolated from the thruster body and exhibit distinct floating potential, the discharge characteristics of the thruster change.

Based on this consideration, we investigated and discussed the interactions of the pole pieces with the discharge plasma in a 2-kW-class magnetic-layer-type Hall thruster by isolating the surface material of each pole piece from the thruster body.

II. Experimental Apparatus and Procedure

A. Hall Thruster Configurations

To investigate the pole-piece interactions, the breadboard model (BBM) of the 2-kW-class Hall thruster manufactured by IHI Aerospace (shown in Fig. 1) and a commercial hollow cathode (HCN-252, Veeco/Ion Tech) were employed in this study. The discharge channel of the BBM thruster, the effective diameter of which is 100mm, was made of boron nitride. The thruster comprises inner and outer concentric electromagnetic coils, responsible for

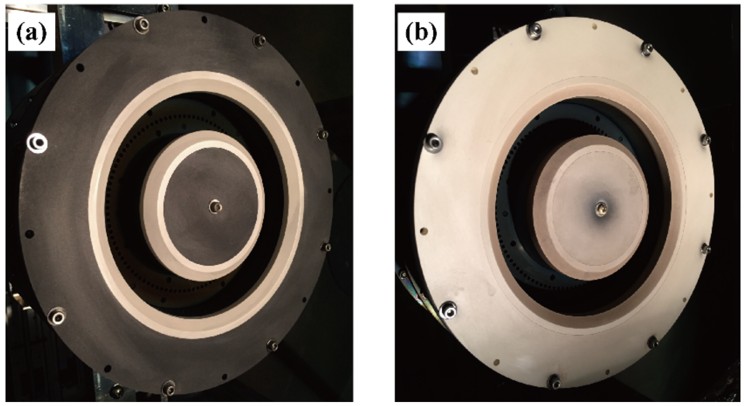

Figure 1. Two boundary conditions of the pole pieces in the 2-kW-class Hall thruster (No.1 configuration). The pole pieces were covered with (a) graphite, and (b) boron nitride.

Table 1. Thruster configurations.

Configuration number	Discharge channel taper	Shape of gas distributor at anode
1	Shallow	Orifice
2	Shallow	Slit
3	Deep	Orifice

inducing the magnetic field in the thruster. The hollow cathode was mounted externally.

The pole pieces were covered by graphite because of high resistance to ion sputtering, and the graphite covers were electrically isolated from the thruster body. In addition, a dielectric material (boron nitride) was employed as the pole-piece cover, as shown in Fig. 1(b), to evaluate the effects of the boundary conditions of the pole pieces on the thruster. Furthermore, two discharge channels (shallow/deep taper at the channel exit) and two anodes (slit/orifice type gas distributor) were employed to evaluate the mutual interaction between the thruster configuration and the boundary conditions of the pole pieces. Table 1 lists three thruster configurations with their corresponding configuration numbers.

B. Experimental Setup and Condition

The experiments were conducted in a vacuum chamber, the diameter and length of which were 2 m and 5 m, respectively. The chamber was located in the Institute of Space and Astronautical Science and had been used to conduct endurance tests of HAYABUSA's ion thrusters [5]. Four cryopumps, each with a diameter of 76 cm, were attached to the chamber. The pressure within the vacuum chamber was maintained at 4.0×10^{-3} Pa when the total xenon flow rate of 7.7 mg/s was fed to the anode and cathode during the experiment.

Figure 2 shows the electrical circuit of the experiment. The anode, keeper, and heater power supplies were located separately from the ground to prevent the neutralization of the ion beam through the vacuum chamber wall. The inner and outer coils were connected to each power supply and their negative terminals were grounded. The power supplies were connected outside the vacuum chamber.

Research-grade xenon (99.995% pure), which served as the propellant for adjusting the flow rates, was fed to the anode and cathode using mass flow controllers (SEC-E40, HORIBA STEC). The uncertainly in the mass flow controllers with regard to the anode and cathode were ±0.1 mg/s and ±0.02 mg/s, respectively. The cathode flow rate was maintained at 10% of the anode mass flow rate.

The thrust was measured using a pendulum-type thrust stand with an LED displacement sensor. The thrust stand was calibrated using measured masses on a pulley system connected to a stepping motor stage. To minimize the measurement error due to the thermal drift, the thrust stand zero (the displacement sensor output corresponding to no load condition) was measured for each thrust measurement. The discharge current was measured using a current probe with a Hall sensor (3273-50, HIOKI). The uncertainly in the current measurement was ±1.0% of its reading and ±0.01A.

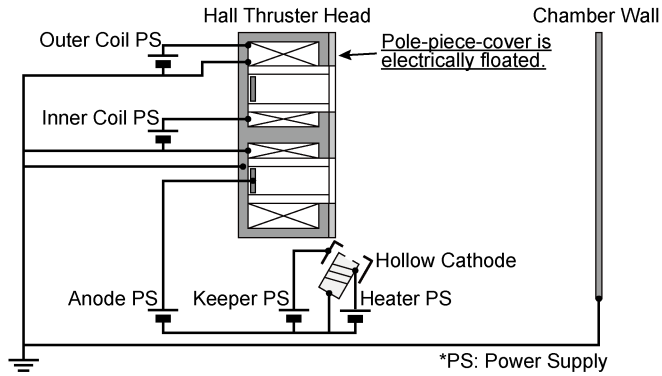

Figure 2. Electrical circuit of the Hall thruster operation.

III. Results and Discussion

A. Floating Potential under Conductor Boundary Condition

As mentioned in chapter 1, both the inner and outer pole-piece covers were isolated from the thruster body. Thus, each cover has its own floating potential. Figure 3 shows the potentials on the pole-piece covers, keeper, and cathode tube as a function of the discharge voltage for various anode mass flow rates under the No.1 configuration and graphite boundary condition. The effects of the anode mass flow rate and discharge voltage on the potentials of the keeper and cathode tube are small. Figures 3(a) and 3(b) show that the keeper discharge and the coupling between the hollow cathode and the ion beam are independent of the operating conditions.

In contrast to the cathode potentials, the potentials on the inner and outer covers decrease with the increases in the anode mass flow rate and discharge voltage. Moreover, the negative potential on the outer cover is greater than that on the inner cover, as shown in Figs. 3(c) and 3(d). The floating potentials of the inner and outer covers vary because of the increase in the electron temperature near the pole pieces, which is in turn due to the increase in the discharge voltage. The neutral number density of xenon increases with the increases in the anode and cathode mass flow rates. An increase in electron-neutral collisions near the pole pieces is due to the increase in the neutral number density. Consequently, the increase of the collisions seems to facilitate the electron transport to the pole pieces, and subsequently, the cover potentials become increasingly negative to repel the electrons from the pole piece. The data presented in Figs. 3(c) and 3(d) suggest that the electron mobility near the outer pole piece is higher than that near the inner pole piece in a magnetic-layer-type Hall thruster with an externally mounted hollow cathode. Furthermore, at a low discharge voltage and a low anode mass flow rate, the potential of the inner pole piece is positive and tends to zero, as shown in Fig. 3(c); this attracts the electrons because of the low electron mobility near the inner pole piece.

B. Discharge Characteristics under the Two Boundary Conditions

Figure 4 shows the discharge characteristics of the Hall thruster as a function of the normalized magnetic field under the two boundary conditions and with the No. 2 configuration; the discharge voltage is 300 V and the anode mass flow rate is 7.0 mg/s. The amplitude of the discharge current oscillation, Δ, shown in Fig. 4(b), is defined as follows.

$$\Delta = \frac{R.M.S.}{\overline{I_d}} = \frac{1}{\overline{I_d}}\sqrt{\frac{\int_0^{\tau}(I_d - \overline{I_d})^2 dt}{\tau}}, \quad \text{where } \overline{I_d} = \frac{\int_0^{\tau} I_d dt}{\tau}, \tag{1}$$

and I_d and τ are the discharge current and measurement time, respectively [6]. The cathode mass flow rate was excluded from the calculation of the specific impulse. Because of constant anode mass flow rate, the effects of the magnetic field on the specific impulse and thrust are similar. In addition, the power consumptions of the magnetic coils and the hollow cathode were excluded from the calculation of the thrust-to-power ratio.

Regardless of the boundary condition, the discharge current and its oscillation have a local minimum at a normalized magnetic field of approximately 0.6, and thereafter, increase with the increase in the normalized magnetic field. The cathode-to-ground voltage (potential difference between the cathode tube and the ground) decreases with

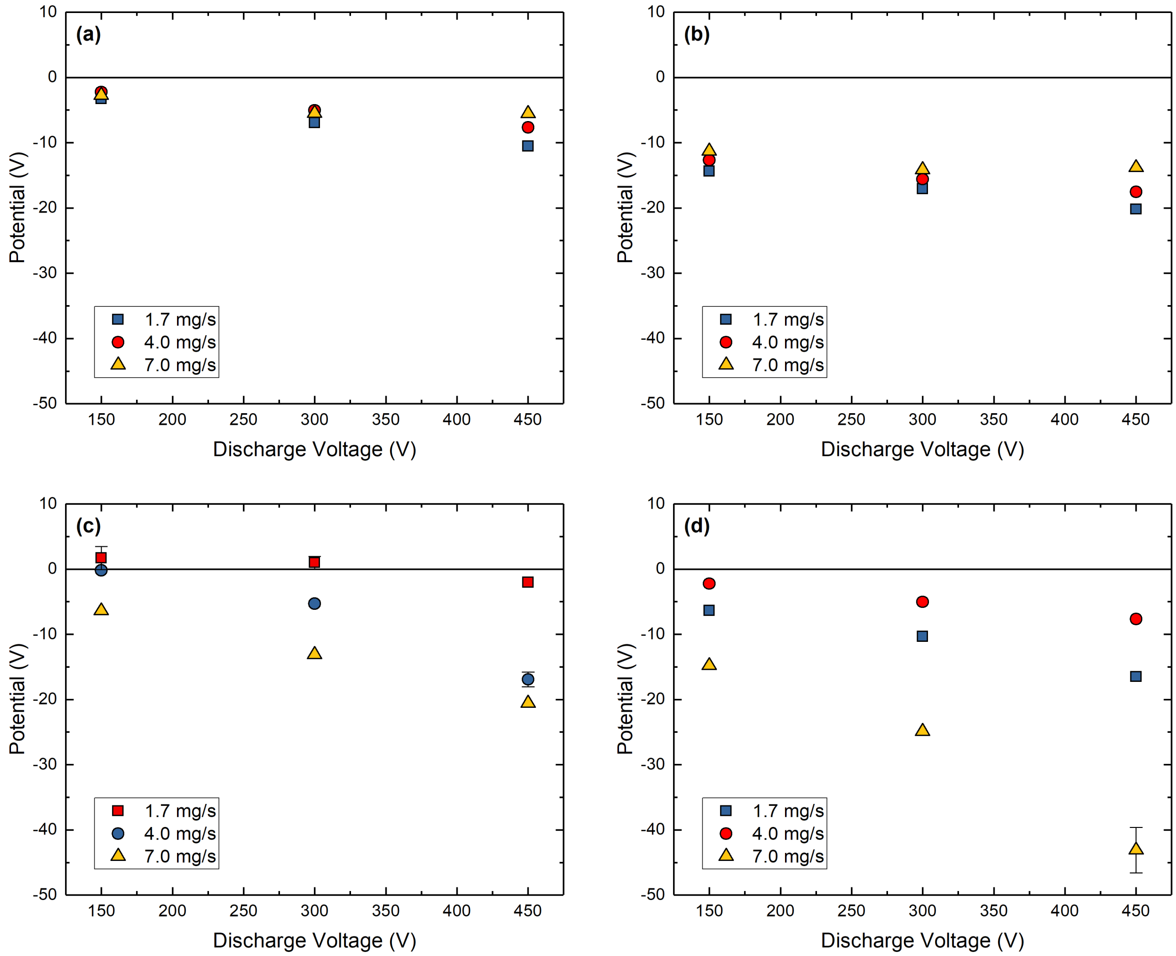

Figure 3. Various potentials associated with the Hall thruster as a function of discharge voltage for different anode mass flow rates under the No.1 configuration, conductor boundary condition, and the magnetic field at which the anode efficiency is maximum: (a) Keeper, (b) cathode tube, (c) inner pole-piece cover, and (d) outer pole-piece cover. Each potential refers to the vacuum chamber potential. The symbols represent the average values of three measurements and the error bars show the standard deviation.

the increase in the normalized magnetic field under both boundary conditions. In addition, the thrust and specific impulse slightly increases with the increases in the normalized magnetic field and remains constant under the effect of a strong magnetic field. Because the effect of the magnetic field on the discharge current is greater than that on the thrust, the thrust-to-power ratio and anode efficiency are maximized at a normalized magnetic field of approximately 0.6 under both boundary conditions. The data presented in Fig. 4 reveal that the trends in the discharge behavior and thrust performance with respect to the magnetic field strength remain unaffected by the boundary conditions of the pole pieces. However, the thrust performance at constant magnetic field strength was slightly affected by the boundary conditions.

C. Thrust Performance Comparison under the Two Boundary Conditions

Table 2 presents the comparison of the thrust performance obtained under two boundary conditions for various thruster configurations and under the magnetic field at which the anode efficiency is maximum. The discharge current under the graphite condition is lower than that under the boron nitride condition in most cases of the thruster configurations and operating conditions, as listed in Table 2. On the other hand, the change in the boundary condition tends to affect the thrust and specific impulse. However, changing the boundary condition from boron nitride to graphite improves the thrust-to-power ratio and anode efficiency in most cases, because of the considerable decrease in the discharge current.

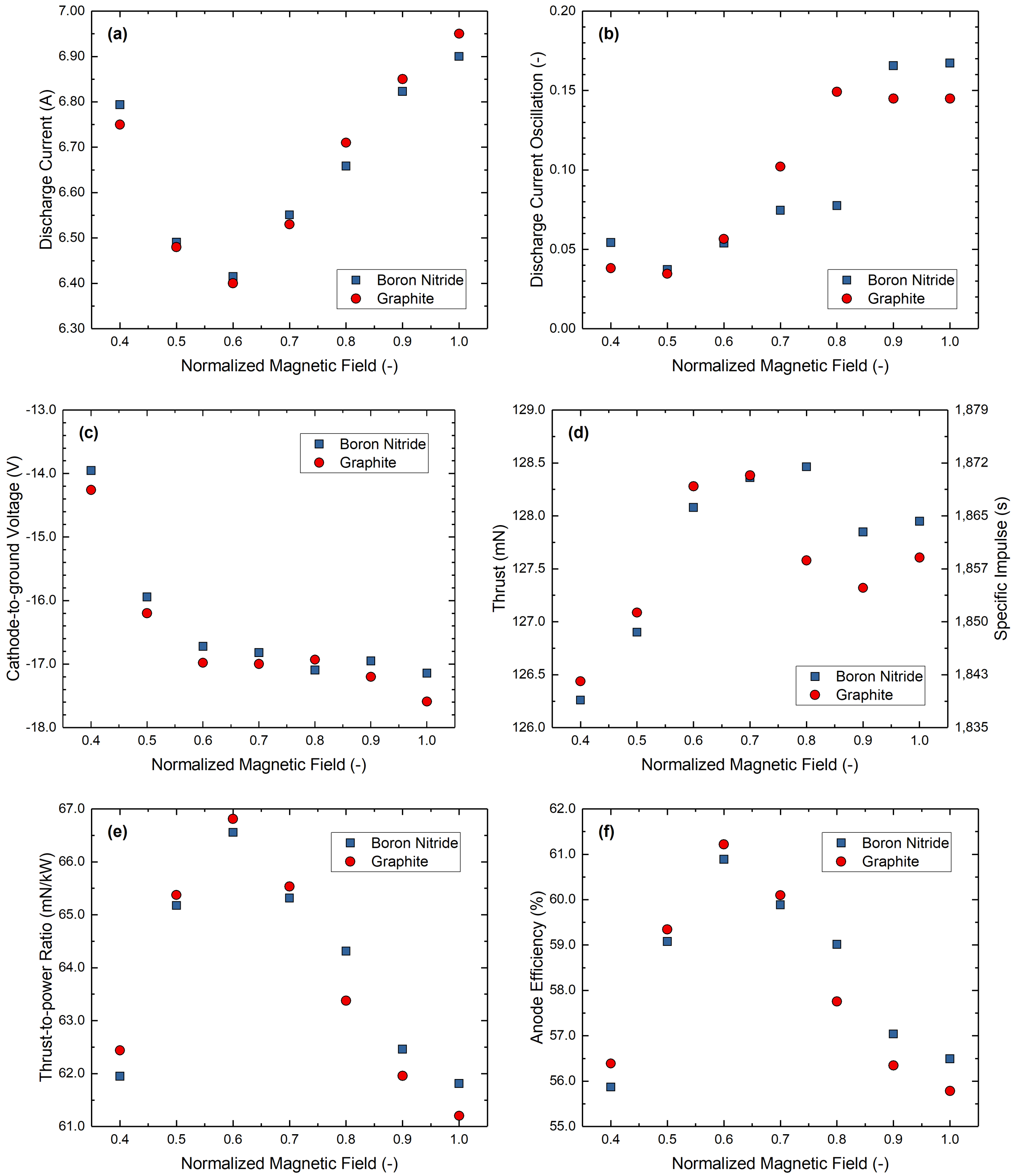

Figure 4. Different parameters associated with the Hall thruster as a function of normalized magnetic field under the two boundary conditions and with the No. 2 configuration for a discharge voltage of 300 V and an anode mass flow rate of 7.0 mg/s: (a) Discharge current, (b) discharge current oscillation, (c) cathode-to-ground voltage, (d) thrust (specific impulse), (e) thrust-to-power ratio, and (f) anode efficiency.

Table 2. Comparison of thrust performance obtained under the two boundary conditions for various thruster configurations and under a magnetic field at which the anode efficiency is maximum. The columns "B" and "G" represent the values of the parameters obtained under the boron nitride boundary and graphite boundary, respectively. The "diff." column represents the difference between the values of the parameters obtained under the graphite boundary and those obtained under the boron nitride boundary. The negative values are highlighted in red.

V_d, V	$\dot{m}_a$, mg/s	Config.	I_d, A			F, mN (I_{sp}, s)			F/P, mN/kW			η_a, %		
			B	G	diff.	B	G	diff.	B	G	diff.	B	G	diff.
150	1.7	No. 1	1.25	1.24	-0.01	12.1 (728)	12.6 (753)	0.5 (25)	64.8	67.4	2.6	23.2	24.9	1.7
		No. 3	1.14	1.10	-0.04	10.7 (644)	10.6 (638)	-0.1 (-6)	62.9	64.2	1.3	19.9	20.1	0.2
	4.0	No. 1	3.79	3.38	-0.41	39.2 (998)	37.5 (955)	-1.7 (-43)	68.9	73.9	5.0	33.7	34.6	0.9
		No. 3	3.54	3.48	-0.06	37.4 (954)	36.6 (934)	-0.8 (-20)	70.6	70.3	-0.3	33.0	32.2	-0.8
	7.0	No. 1	6.87	6.64	-0.23	76.6 (1115)	77.8 (1133)	1.2 (18)	74.3	78.2	3.9	40.6	43.4	2.8
		No. 3	6.87	6.64	-0.23	78.3 (1140)	77.1 (1123)	-1.2 (-17)	76.0	77.4	1.4	42.5	42.6	0.1
300	1.7	No. 1	1.58	1.48	-0.10	25.5 (1527)	25.4 (1522)	-0.1 (-5)	53.8	57.0	3.2	40.3	42.6	2.3
		No. 3	1.33	1.30	-0.03	22.9 (1373)	22.0 (1319)	-0.9 (-54)	57.5	56.3	-1.2	38.7	36.4	-2.3
	4.0	No. 1	3.36	3.23	-0.13	65.6 (1671)	66.0 (1682)	0.4 (11)	65.0	68.1	3.1	53.2	56.2	3.0
		No. 3	3.73	3.66	-0.07	66.3 (1691)	65.0 (1657)	-1.3 (-34)	59.3	59.3	0.0	49.2	48.2	-1.0
	7.0	No. 1	6.45	6.31	-0.14	130.4 (1899)	132 (1923)	1.6 (24)	67.4	69.8	2.4	62.8	65.8	3.0
		No. 2	6.53	6.41	-0.12	129.9 (1892)	128.5 (1871)	-1.4 (-21)	66.3	66.8	0.5	61.5	61.3	-0.2
		No. 3	6.16	6.04	-0.12	121.8 (1774)	122.8 (1788)	1.0 (14)	65.9	67.8	1.9	57.3	59.4	2.1
450	1.7	No. 1	1.66	1.60	-0.06	33.7 (2023)	33.4 (2005)	-0.3 (-18)	45.2	46.4	1.2	44.8	45.6	0.8
		No. 3	1.25	1.21	-0.04	25.9 (1553)	25.0 (1500)	-0.9 (-53)	46.2	45.8	-0.4	35.1	33.7	-1.4
	4.0	No. 1	3.43	3.72	0.29	80.6 (2054)	87.2 (2222)	6.6 (168)	52.3	52.1	-0.2	52.7	56.8	4.1
		No. 3	3.48	3.42	-0.06	78.0 (1988)	76.4 (1948)	-1.6 (-40)	49.8	49.6	-0.2	48.5	47.4	-1.1
	7.0	No. 1	6.81	6.57	-0.24	164.4 (2396)	164.9 (2402)	0.5 (6)	53.7	55.7	2.0	63.1	65.7	2.6
		No. 3	6.43	6.06	-0.37	152.7 (2225)	149.1 (2172)	-3.6 (-53)	52.8	54.6	1.8	57.5	58.2	0.7

Paterson et al. discussed the effects of the electrical configurations and boundary conditions on the length of the ionization and acceleration regions using the power spectrum density of the discharge current [4]. Fife et al. [7] first described the breathing mode oscillation of a Hall thruster using the following relationship:

$$2\pi f_i = \frac{\sqrt{V_i V_n}}{L_d}, \tag{2}$$

where f_i is the primary oscillation frequency of the Hall thruster, V_i is the accelerated ion velocity at the exit of the acceleration region, V_n is the thermal velocity of the neutral propellant entering the ionization region, and L_d is the length of the ionization and acceleration regions. The ion velocity and thermal neutral velocity are assumed to be approximately constant under each operating condition, because the ion velocity depends on the discharge voltage and the neutral velocity depends on the discharge power. Based on the assumption, a change in the primary oscillation frequency may indicate a change of the discharge length in the channel.

Figure 5 shows the typical power spectrum density of the discharge current. The power spectrum density was obtained using the fast Fourier transform (FFT) method and the measured discharge current oscillation. The primary oscillation frequencies under both the boundary conditions are the same, i.e., 34 kHz; in addition, the amplitudes remain approximately the same, as shown in Fig. 5.

Figure 6 shows the relationship between the change in the anode efficiency (listed in Table 2) and the change in the primary oscillation frequency under various operating conditions. The vertical and horizontal axes represent the differences in the anode efficiencies and in the primary oscillation frequencies obtained under the graphite and boron nitride boundary conditions, respectively. Except under a few operating conditions, the surface condition of the pole piece does not affect the primary oscillation frequency, as shown in Fig. 6. Moreover, there is no clear correlation between the change in the anode efficiency and the change in the primary oscillation frequency. These results indicate that the suppression of the discharge current and the improvement in the thrust performance, as presented in Table 2, are not only because of the change in the discharge phenomenon in the ionization and acceleration regions but also because of other mechanisms near the pole pieces.

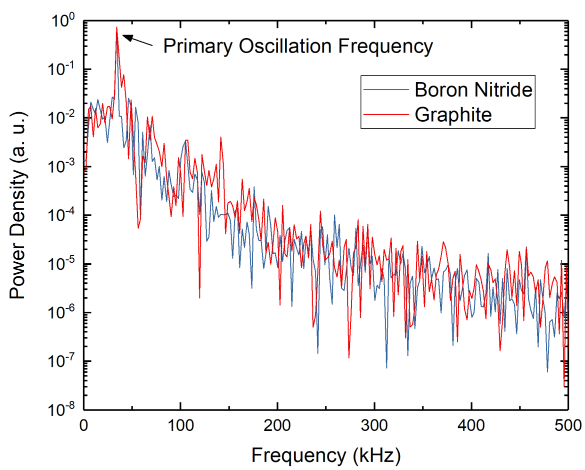

Figure 5. Power spectrum density of the discharge current under the two boundary conditions and with the No. 1 configuration for a discharge voltage of 450 V and an anode mass flow rate of 7.0 mg/s.

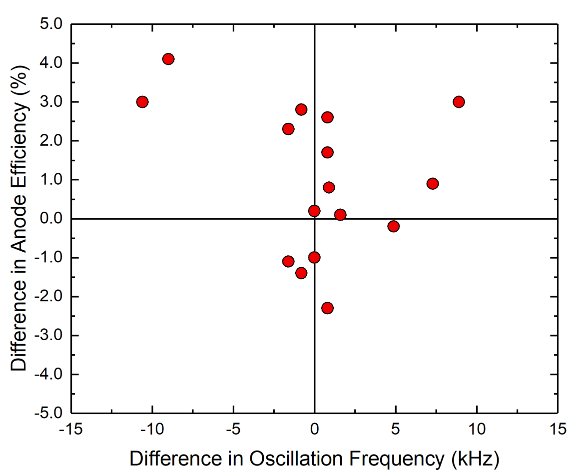

Figure 6. Relationship between the change in the anode efficiency and the change in the oscillation frequency. The vertical and horizontal axes represent the differences in the anode efficiencies and in the primary oscillation frequencies under the graphite and boron nitride boundary conditions, respectively.

Hence, to clarify the mechanism for the performance improvement owing to the change in the boundary condition of the pole pieces, the effects of the boundary conditions on the plasma parameters near the discharge channel and pole pieces will be investigated in the future using a Langmuir probe measurement.

IV.Conclusions

The pole-piece interactions with the discharge plasma in a 2-kW-class BBM Hall thruster (manufactured by IHI Aerospace) with externally mounted commercial hollow cathode were investigated and analyzed. The pole pieces were covered with graphite, and the cover was electrically isolated from the thruster body. In addition, a dielectric material (boron nitride) was employed as the pole piece cover to evaluate the effects of the boundary condition of the pole piece. The following are the experimental results of this study:

At a constant magnetic field strength, the floating potentials of the conductive pole-piece covers decrease with the increases in the anode mass flow rate and discharge voltage. Moreover, the negative potential on the outer cover is greater than that on the inner cover. These results suggest that the electron mobility near the outer pole piece is higher than that near the inner pole piece in a magnetic-layer-type Hall thruster with an externally mounted hollow cathode. Furthermore, the electron mobility near the pole pieces is affected by the anode mass flow rate and discharge voltage.

The trends in the discharge behavior and thrust performance with respect to the magnetic field strength remain unaffected by the boundary conditions of the pole pieces. However, the thrust performance at constant magnetic field strength was slightly affected by the boundary conditions. On the basis of the thrust performance comparison in terms of the two boundary conditions with the magnetic field at which the anode efficiency is maximum, the discharge current under the conductor boundary condition is lower than that under the dielectric boundary condition in most cases of the thruster configurations and operating conditions. In contrast to the discharge current behavior, the change in the boundary condition tends to affect the thrust and specific impulse. However, because of the large decrease in the discharge current, changing the boundary condition from boron nitride to graphite improves the thrust-to-power ratio and anode efficiency in most cases. The FFT analysis of the discharge current oscillation indicates that the suppression of the discharge current was not only because of the change in the discharge phenomenon in the ionization and acceleration regions, but also because of other mechanisms near the pole pieces.

Thus, to clarify the mechanism for the performance improvement owing to the change in boundary condition of the pole pieces, we will investigate the effects of the boundary conditions on the plasma parameters near the discharge channel and pole pieces as a future work.

Acknowledgments

The authors thank Prof. H. Kuninaka, Dr. K. Nishiyama, Dr. S. Hosoda, and Dr. R. Tsukizaki for technical support provided in performing the thrust performance measurements at the Institute of Space and Astronautical Science.

References

[1] Funaki, I., Iihara, S., Cho, S., Kubota, K., Watanabe, H., Fuchigami, K., and Tashiro, Y., “Laboratory Testing of Hall Thrusters for All-electric Propulsion Satellite and Deep Space Explorers,” 52nd Joint Propulsion Conference, AIAA 2016-4942, 2016.

[2] McDonald, M., “Electron Transport in Hall Thrusters,” Doctoral Dissertation in the University of Michigan, 2012.

[3] Goebel, D., Jorns, B., Hofer, R., Mikellides, I., and Katz, I., “Pole-piece Interactions with the Plasma in a Magnetic Shielded Hall Thruster,” 50th Joint Propulsion Conference, AIAA 2014-3899, 2016.

[4] Paterson, P., Kamhawi, H., Huang, W., Yim, J., Herman, D., Williams, G., Gilland, J., and Hofer, R., “NASA HERMeS Hall Thruster Electrical Configuration Characterization,” 52nd Joint Propulsion Conference, AIAA 2016-5027, 2016.

[5] Kuninaka, H. Funaki, I., Shimizu, Y., and Toki, K. “Status on Endurance Test of Cathode-Less Microwave Discharge Ion Thruster,” 34th Joint Propulsion Conference, AIAA 98-3647, 1998.

[6] Yamamoto, N., Komurasaki, K., and Arakawa, Y., “Discharge Current Oscillation in Hall Thrusters,” Journal of Propulsion and Power, Vol. 21, No. 5, pp. 870-876, 2005.

[7] Fife, J., Matrinez-Sanchez, M., and Szabo, J., “A Numerical Study of Low-Frequency Discharge Oscillations in Hall Thrusters,” 33rd Joint Propulsion Conference, AIAA 1997-3052, 1997.